Multi-GNSS implementation and assessment of the phase residual method for structures dynamic load and natural frequency estimation

Marco Mendonça[1], Emerson P. Cavalheri[1], Ana P. Larocca[2], Marcelo C. Santos[1]

[1] University of New Brunswick, 15 Dineen Dr, Fredericton, NB, Canada (marco.mendonca@unb.ca)
[2] São Paulo University, Av. Trab. São Carlense, 400, São Carlos, SP, Brazil.

Key words: *GNSS, Phase-Residuals, Double-Difference, Multipath, Natural Frequency, Structure Monitoring*

ABSTRACT

Continuous monitoring of the dynamic displacement of bridges is usually accomplished with the use of traditional displacement measurement dedicated equipment, such as accelerometers and displacement transducers. During the past decade, following the increase in quality of GNSS equipment, new methodologies were developed to provide equivalent types of measurements at a lower cost. One of these methods is the phase residuals method (PRM), where the phase residuals from a relative static GPS positioning are assessed in the frequency domain. This paper investigates the limitations imposed to the method and how the use of modernized GNSS signals may improve the reach of applications of the PRM. This study concludes that the multipath frequency influence in the power spectrum is less prominent in modernized GNSS signals, thus, extending the reach of the method for sub-Hz natural and displacement frequencies estimation.

I. INTRODUCTION

Structure monitoring is a paramount activity for both private and public entities involved in civil construction. In order to ensure a safe and continuous service, methods to assess possible structure deterioration, as well as comparisons with nominal characteristics are often performed in the most diverse contexts. The estimation of dynamic load displacement and natural frequencies in structures, especially bridges, may indicate structural deterioration or even point to errors in load and deformation calculations. Generally, vibration tests are performed using accelerometers or other types of transducers. In the past decades, the use of Global Navigation Satellite Systems (GNSS) has been introduced into this scope (Psimoulis et al., 2008; Yi et al., 2013; Yigit et al., 2016; Vazquez et al., 2017; Xi et al., 2018).

GNSS signals, in general, follow a standard composition with a code component modulated into a carrier-phase component. The code component, being a modulated signal carrying information, has an accuracy on the meter level for range measurements. On the other hand, the carrier-phase, working on a much higher frequency, has a millimeter to centimeter level precision. With this scenario in mind Schaal et al. (2002), developed the phase-residuals method (PRM) for structure deformation monitoring. This method is based on the spectral analysis of the residuals of the double-difference between two receivers and two satellites. Methods analyzing the spectrum of the GPS/GNSS derived time series of coordinates are well-covered in literature. The PRM on the other hand, relies only on the double-difference observation residuals, mathematically eliminating several concerns found in precise coordinate determination.

In this paper, the PRM is extended from the use of single frequency GPS datasets to the use of modernized GNSS signals on the double-differencing procedure. Since different constellations and different signals have different power and modulation characteristics, this paper explores differences in the frequency domain to assess possible improvements to the method.

This paper is divided into the following sections: related work structural load displacement and natural frequency assessment, focusing on bridges, the PRM, and characteristics of the modernized GNSS signals, followed by two experiments, their results, and finally, concluding remarks.

II. RELATED WORK

A. *Natural frequency assessment*

The estimation of the bridge's platform natural frequency is a task performed during both planning and after construction phases. Its estimation is of the utmost importance to ensure structural integrity and the comfort of the users. A few authors have touched the subject over time.

Huang et al. (1992), analyzes natural frequencies of five types of cable-stayed bridges: Continuous beam, single cantilever, T-shaped frame, T-shaped continuous frame and finally radial type. The natural frequencies found vary between 0.646 Hz, for the single cantilever type, up to 6.012 Hz for the T-shaped continuous frame type.

Mashaly et al. (2013), utilizes a response spectrum methodology to model and estimate the natural frequency of beam-supported footbridges with span values varying from 15 m to 35 m. After testing two modelling methodologies that agree on the hundredth of Hz level, the authors found that the natural

frequencies may vary between 3.24 Hz for the 35 m span bridge, up to 6.71 Hz for the 15 m span bridge.

Ito (1991), developed an approximation for cable-stayed bridges in Japan:

$$\mathrm{f_{nat}}=100/\mathrm{L}, \quad (1)$$

where L represents the bridge span. It is possible to see that the equation provides a rough approximation to actual values when comparing the results from footbridges by Mashaly et al. (2013), with a more complex model, and Ito (1991). Table 1 provides an overview of both natural frequency estimation methods:

Table 1. Natural frequency estimation comparison

Bridge span (m)	Mashaly et al. (2013) (Hz)	Ito (1991) (Hz)
15	6.71	6.67
20	5.21	5.00
25	4.42	4.00
30	3.78	3.34
35	3.24	2.85

Even though both methodologies approach structures with different support methods, the magnitude of the natural frequencies are similar for the same spans on a 0.5-Hz level. For the purposes of this article, the approximation by Ito (1991) will be utilized.

B. *The Phase-Residual Method*

The PRM is based on the analysis of GPS carrier phase double-difference residuals (Schaal et al. , 2002). Considering Equation 2 as the fundamental carrier-phase equation:

$$\varphi_R^1 = \rho_R^1 - c(dt_R - dt^1) + \cdots \\ T_R^1 - I_R^1 + \lambda N_R^1 + m + \epsilon \quad (2)$$

where ρ_R^1 is the geometric distance between satellite 1 and receiver R, dt are the clock biases, T is the tropospheric induced delay, I is the ionospheric delay, N is the integer ambiguity, m is the multipath effect and finally ϵ are the unmodelled and inherent noises. By performing the double differences between receivers R and S, and satellites 1 and 2, as Equation 3 shows, the resultant mathematical model is represented by Equation 4 (Teunissen at al., 2017).

$$\varphi_{RS}^{12} = (\varphi_S^{12} - \varphi_R^{12}) - (\varphi_{RS}^1 - \varphi_{RS}^2) \quad (3)$$

$$\varphi_{RS}^{12} = \rho_{RS}^{12} + T_{RS}^{12} - I_{RS}^{12} + \lambda N_{RS}^{12} + m + \epsilon, \quad (4)$$

On Equation 4, the terms T_{RS}^{12} and I_{RS}^{12}, are the residual tropospheric and ionospheric delay, respectively. Considering short baselines between the reference and the rover antenna (<1 km), those terms become negligible. The resultant is equation 5:

$$\varphi_{RS}^{12} = \rho_{RS}^{12} + \lambda N_{RS}^{12} + m + \epsilon, \quad (5)$$

where the parameters ρ_{RS}^{12} and λN_{RS}^{12} represent the geometric relation between both receivers and satellites, while ϵ represents the system noise floor and m the multipath error. The latter component is of high importance in this measurement, since it is a difficult quantity to estimate or correct. Nowadays, three main techniques for multipath mitigation are the most widely adopted (Teunissen at al., 2017):

- The use of co-centric choke rings around the antenna, creating an area of high-impedance thus preventing the propagating of surface reflected waves;
- A stealth ground plane, composed of a high radially increasing sheet resistive from the antenna element to the end of the ground plane, also blocking surface reflected signals;
- A pin-wheel antenna following the same principle as the choke-ring antenna, but with a printed resistive patter instead of bulky rings.

In order to properly assess and extend the use of the PRM as this paper proposes, it is important to notice that besides the aforementioned multipath mitigation strategies, all the remaining multipath effects will be included in the phase double-difference measurements and consequently to the residuals vector as Equation 5 shows.

Finally, assuming the short baseline scenario and the adoption of multipath mitigation techniques, the PRM requires the spectral analysis of said residuals in order to estimate its frequency components through a Fast-Fourier Transform (FFT).

Practical applications of the method were performed in several scenarios. In Larocca et al. (2005), the Pierre-Laporte bridge in Quebec City, Canada, was surveyed and the PRM applied and compared to a spectral analysis on the station height, rather than the residuals. In this study, the largest baseline was of 1 km, enabling the mathematical model to be reduced to Equation 5 in both methods. With a center span of 667 m, the expected natural frequency of the bridge is on the sub-Hz magnitude. The results of the spectral analysis are presented in Figures 1 and 2.

The peak value for the height time series analysis method was 0.2117 Hz, and 0.2176 Hz for the PRM. It is important to mention that even though both methods were found to be equivalent in terms of estimating the bridge's natural frequencies, the PRM is shown to be more versatile since it does not rely on the precise estimation of the rover antenna positions, hence, not being affected by a lack of satellite visibility or poor geometric conditions.

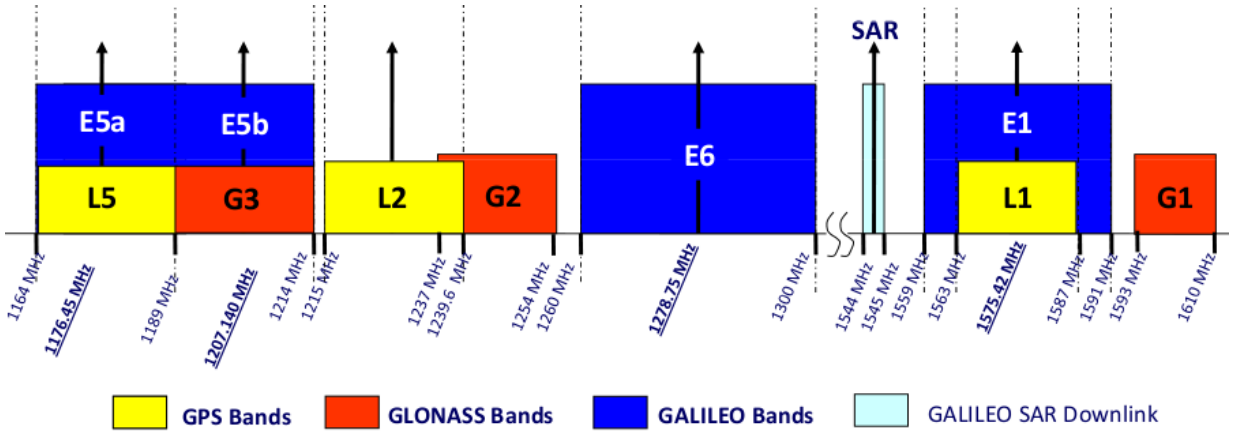

Figure 3. GNSS signals from the GPS, GLONASS and Galileo constellations.

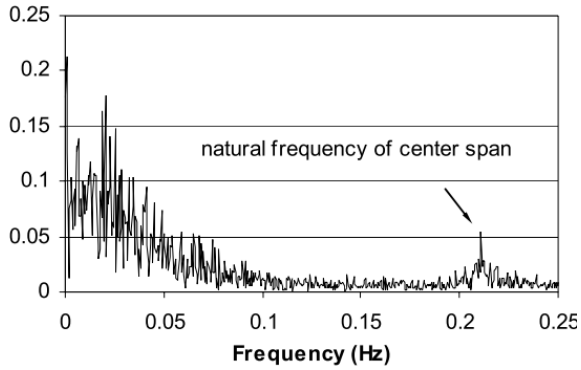

Figure 1. FFT applied to the antenna height component

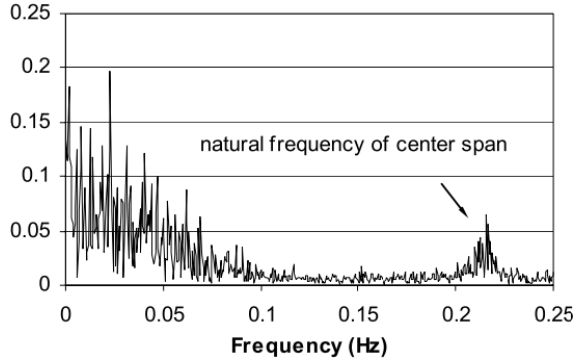

Figure 2. FFT applied to the double-difference phase residuals

C. *Modernized GNSS Signals*

Since the advent of satellite positioning systems, a steady progress in terms of satellites and constellations available has been made throughout the world. Nowadays, six different constellations are available for civilian use, each one with different signals and characteristics. For clarity purposes, this study will focus in three constellations: The Global Positioning System (GPS), developed and operated by the United States, the *Globalnaya Navigatsionnaya Sputnikovaya Sistema* (GLONASS) developed by the former Soviet Union and today operated by Russia, and the Galileo system, developed and operated by the European Union. Figure 3 shows an overview of the spectrum allocation for each GNSS signal (Subirana et al., 2011).

Considering here the effects of multipath on GNSS positioning and double-differences, Strode et al. (2016) and Hilla et al. (2002) derived Equations 6 to estimate the effects of multipath on each frequency by the means of the pseudorange and carrier-phase measurements.

$$MP1 \equiv p_1 - \left(1 + \frac{2}{\alpha - 1}\right)\phi_1 + \left(\frac{2}{\alpha - 1}\right)\phi_2$$

$$MP2 \equiv p_2 - \left(\frac{2\alpha}{\alpha-1}\right)\phi_1 + \left(\frac{2\alpha}{\alpha-1} - 1\right)\phi_2 \qquad (6)$$

$$MP5 \equiv p_5 - \left(\frac{2}{\alpha-1}\right)\phi_1 + \left(\frac{2\alpha}{\alpha-1} - 1\right)\phi_5,$$

where $p_n \; and \; \phi_n$ are, respectively, the pseudorange and carrier-phase measurement of frequency n, and α is the ratio between the frequencies of both signals on the equation. For MP1 and MP2,

$$\alpha \equiv \left(\frac{f_1}{f_2}\right)^2 \qquad (7)$$

and for MP5,

$$\alpha \equiv \left(\frac{f_1}{f_5}\right)^2, \qquad (8)$$

Where Table 2 shows the frequencies for each signal considered in this study.

Table 2. GNSS signals centre frequencies analysed

Constellation	Freq. 1 (GHz)	Freq. 2 (GHz)	Freq. 5 (GHz)
GPS	1.57542	1.2276	1.17645
GLONASS	1.6015	1.2455	-
Galileo	1.57542	-	1.17645

Since Equations 6 to 8 show that multipath is a function of the frequency values, and independent

measurements on each signal, the multipath behaviour is also expected to be different on each signal.

III. EXPERIMENTS AND RESULTS

Two experiments were conducted in this paper, the zero baseline and oscillating platform. The zero-baseline experiment provided a reference for the PRM assessment on different frequencies, since there is no movement or physical difference between the measurements of both receivers. The oscillating platform, on the other hand, proves the capability of applying the PRM in all modernized GNSS signals.

Both experiments used a pair of JAVAD TRIUMPH-LS receivers, with capabilities of tracking L1, L2 and L5 frequencies for multiple GNSS constellations. In the second experiment, the tactical INS KVH TG6000 was used as benchmark to the PRM. In the sequence, the zero baseline and oscillating platform experiments are detailed.

A. *Zero-baseline experiment*

The zero-baseline experiment consisted of two static GNSS receivers collecting data from the same antenna through an externally powered signal splitter. The collection period was 1 hour with an observation rate of 10 Hz. The objective of this experiment was to determine, in the frequency domain, a minimum noise reference from the double-difference phase residuals series between two satellites, one as reference close to zenith and another at a lower elevation angle. Figure 4 shows the reference satellites for each constellation (G26 for GPS, R11 for GLONASS and E25 for Galileo). This particular set of satellites was chosen due to their geometric arrangement, and availability of the modernized L5 signals.

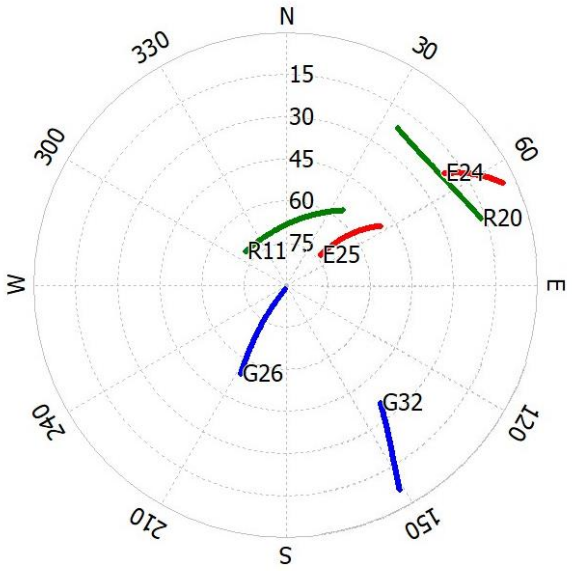

Figure 4. Skyplot of the zero-baseline experiment

With the satellites of Figure 4, the double-differences were computed on all available frequencies shown on Table 2.

Initially, the spectral analysis of the double difference residuals was computed according to the PRM.

Figure 5 to 7 show the results of the double-difference phase-residual power spectrum for the GPS signals L1, L2 and L5, GLONASS L1 and L2, and Galileo E1 and E5a.

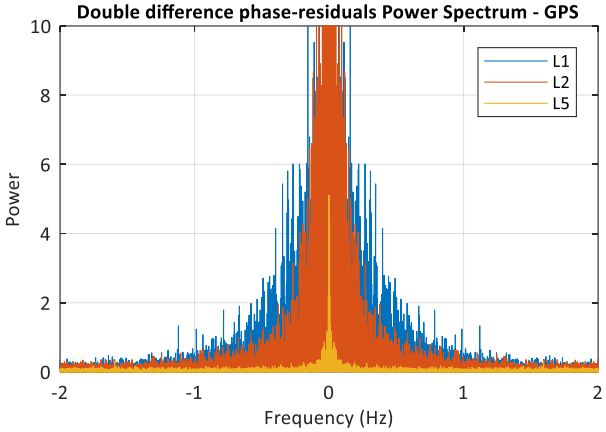

Figure 5. Power spectrum of the GPS constellation

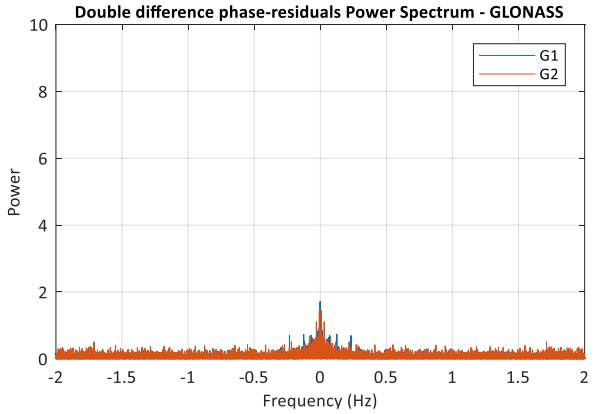

Figure 6. Power spectrum of the GLONASS constellation

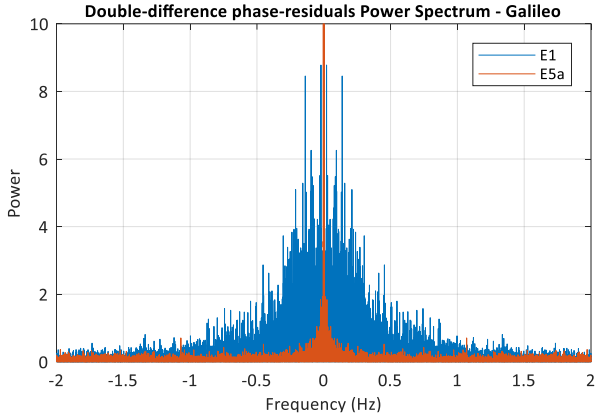

Figure 7. Power spectrum of the Galileo constellation

On Figure 5, it is possible to see the different behaviour of each GPS signal. The peak at the zero frequency represents a constant component of the signal. This offset is assumed to be due to differences

on both splitter outputs, and on impedance differences of the cables used to connect both receivers to the splitter. Furthermore, and more importantly, it is possible to see that the low frequency noise of the L1 component reaches much further than the same noise for L5. Analysing this behaviour through Equation 5, the multipath component appears to be the responsible for such difference. In order to confirm this hypothesis, Figure 8 shows the multipath indexes from Equation 6 for the first 15 minutes of the zero-baseline experiment and for all three GPS frequencies.

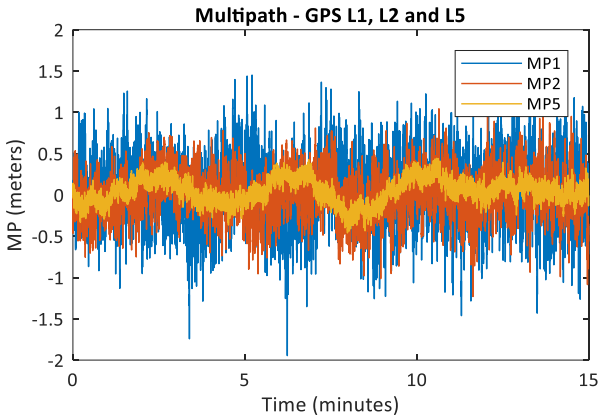

Figure 8. Multipath indexes for the GPS signal

It is possible to see that the MP5 index, corresponding to the multipath effect on L5, is significantly smaller than the same quantity for L1. Another important aspect to be verified is the frequency component of the multipath signature. Figure 9 shows a smoothed line as a result of a low pass filter (moving average, bins of 10 seconds).

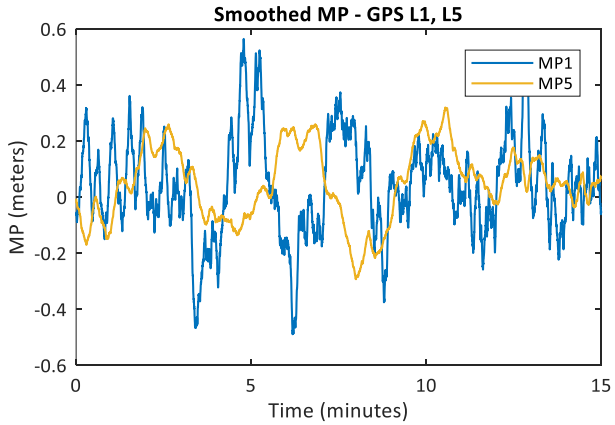

Figure 9. Smoothed multipath for the GPS L1 and L5

On Figure 9, the multipath on L1 shows frequency components ranging from the same as L5, to higher frequencies as well. Figure 10 confirms this behaviour through a spectral analysis of the multipath indexes on L1 and L5.

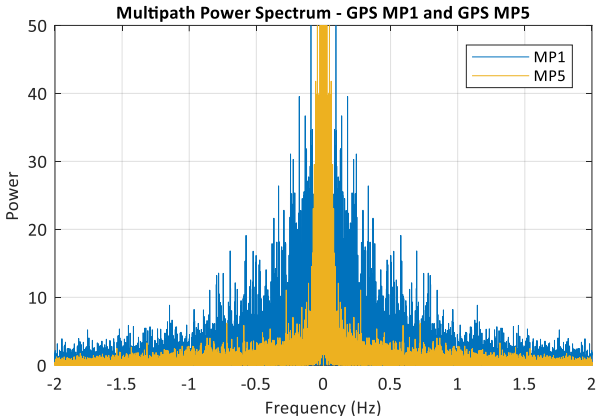

Figure 10. Power spectrum for GPS MP1 and MP5

The behavior of the multipath on L5 points to the conclusion that for the assessment of lower natural or load displacement frequencies under 1 Hz, the residuals of the double-difference on L5 are a more suited measurement than the correspondent for L1. This result confirms the behavior seen on Figure 5.

As for the GLONASS constellation, both frequencies presented virtually the same results in this experiment. A probable cause for this effect is the possibility that the GLONASS signal from satellites R11 and R20 were almost equally affected by multipath, which is approximately the same case as the GPS frequencies L1 and L2. Figure 11 shows the multipath signals on GLONASS G1 and G2.

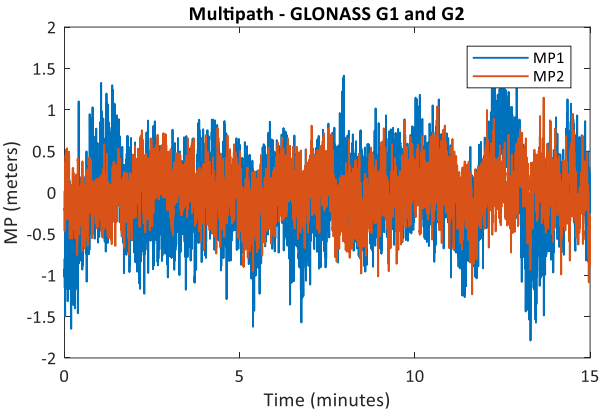

Figure 11. Multipath indexes for the GLONASS signal

Figure 12 shows the spectral analysis for the GLONASS multipath signals. Even though the GLONASS G2 frequency seems to be slight less affected than G1, the noise level introduced by multipath under 0.5 Hz is still significant in both. It is important to notice that in this experiment the multipath effect introduced on GLONASS signals is smaller than the one experience in both GPS and Galileo L1 and E5a. The probable reason for this behavior lies in the fact that the GLONASS constellation has a higher orbital inclination, making it less prone for multipath on average than GPS and Galileo.

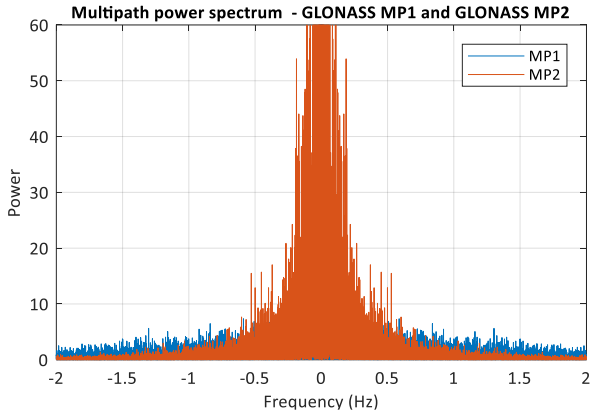

Figure 12. Power spectrum for GLONASS MP1 and MP2

For the Galileo constellation, a conclusion similar to the GPS constellation can be drawn, where the signal E5a is significantly less affected that E1, enabling displacements of lower frequencies to be adequately tracked on the PRM. Figure 13 shows the multipath quantities for E1 and E5a for the first 15 minutes, and Figure 14 shows the spectral analysis for the same frequencies.

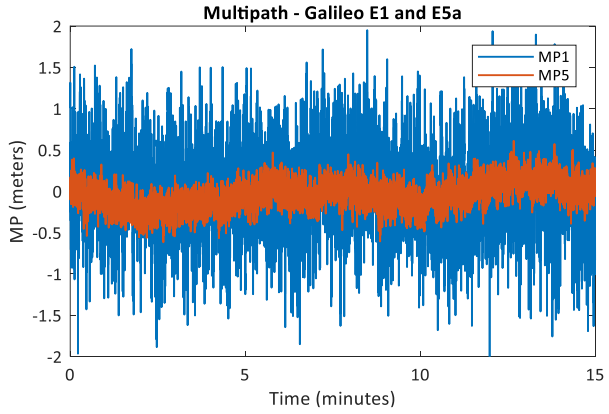

Figure 13. Multipath indexes for the Galileo signal

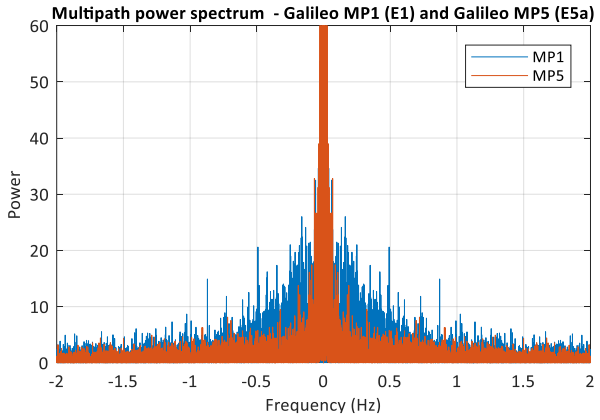

Figure 14. Power spectrum for Galileo MP1 and MP2

Finally, Table 3 shows a summary of the phase residuals RMS for each signal analysed.

Table 3. Double-difference phase residuals RMS

Signal	RMS (cm)
GPS L1	2.009
GPS L2	2.146
GPS L5	0.840
GLONASS G1	0.991
GLONASS G2	1.165
Galileo E1	1.960
Galileo E5a	1.387

B. *Oscillating platform experiment*

For the collection in this experiment, the receivers were setup on an open sky environment. A base receiver was mounted on a tripod collecting 10 Hz static observations throughout the experiment. The oscillating platform had the rover receiver and a tactical INS firmly attached to it. The rover and INS observation rates were 10 Hz and 150 Hz, respectively, and located about 20 m from the base. During the data collection, the platform oscillated on a frequency of 2 Hz. The GNSS base and rover data were processed using the same strategy adopted in the zero-baseline experiment. After the GNSS processing, DD phase residuals of a pair of satellites for GPS, GLONASS, and Galileo, in the frequencies L1, L2 and L5 were obtained as shown on Figure 15.

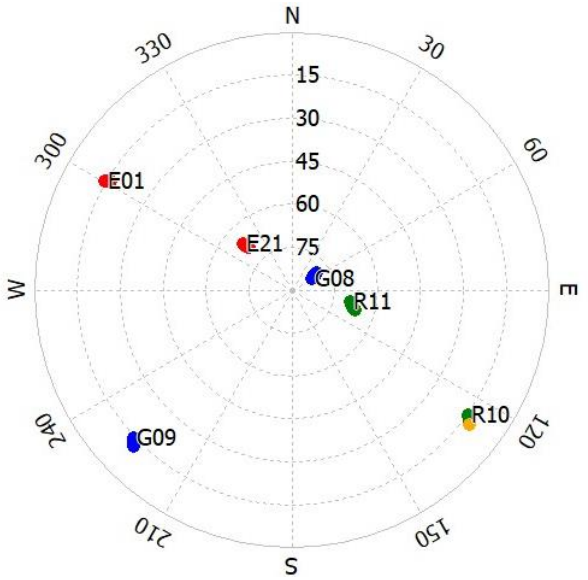

Figure 15. Skyplot of the oscillating platform experiment

Subsequently, by transforming each of the residual series to the frequency domain, a comparison was performed with the tactical INS data.

Figure 16 shows, in the frequency domain, the reference data from the KVH TG6000 INS. The peak was found to be 1.9989 Hz. The discrepancy with the nominal 2 Hz set at the oscillating platform is likely due to inaccuracies on the platform itself, given the high quality and stability of the INS equipment measurements.

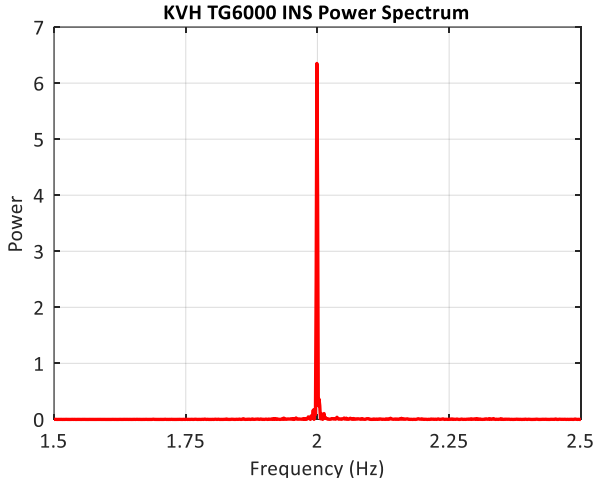

Figure 16. Platform oscillation as measured by the tactical INS

Table 4 shows the peaks found at each one of the analysed GNSS frequencies.

Table 3. Oscillation peak for each GNSS frequency

Signal	Oscillation (Hz)
GPS L1	1.9999
GPS L2	1.9984
GPS L5	1.9989
GLONASS G1	1.9999
GLONASS G2	1.9999
Galileo E1	1.9984
Galileo E5a	1.9991

Finally, Figure 17 shows the behavior of the peak frequency region for GPS L1. Since the 2 Hz frequency lies in a region greater than the multipath interference zone, all signals performed equivalently and the plots very similar for this region.

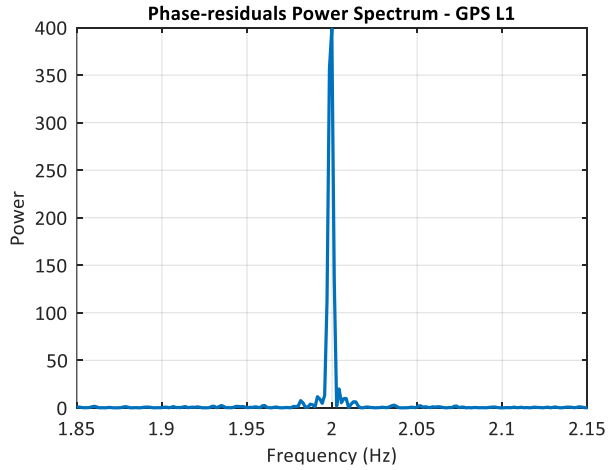

Figure 16. Oscillation on the frequency domain for GPS L1

IV. CONCLUSIONS

In conclusion, the work performed on the zero-baseline experiment showed that the modernized frequencies L5 for GPS and E5a for Galileo, outperformed their pairs GPS L1 and L2 and Galileo E1 on what regards resilience for the higher frequency multipath effects. Considering the natural frequency of bridges approximation by Ito (1991), bridges with spans greater than 100 m, meaning that the natural frequency will lay under 1 Hz, will benefit from the PRM applied on modernized frequencies in the likely presence of multipath.

For planning a bridge monitoring system considering the PRM, the receiver log rate should take into consideration the bridge span and the Nyquist frequency for the upper limit, as Equation 9 shows:

$$f_{log} \geq \frac{200}{L}, \tag{9}$$

where f_{log} is the GNSS receiver log frequency, and L is the bridge span. By applying this equation, the natural frequency of the bridge will likely be well distinguishable on the frequency domain on the PRM. As for the sub-Hz frequencies, the use of the GPS L5 and Galileo E5a frequencies is recommended, since it extends the reach of the method and, as shown on the oscillating base experiment, produces results equivalent to any other GNSS frequency.

References

Hilla, S., & Cline, M. (2002). Evaluating Pseudorange Multipath Effects at Stations in the National CORS Network Evaluating Pseudorange Multipath Effects at Stations in the National CORS Network. *Weikko A. Heiskanen Symposium in Geodesy*, 24. https://doi.org/10.1007/s10291-003-0073-3

Huang, D., & Wang, T. Lo. (1992). Impact analysis of cable-stayed bridges. *Computers and Structures*, *43*(5), 897–908. https://doi.org/10.1016/0045-7949(92)90304-I

Ito, M. (1991). *Cable-stayed bridges : Recent developments and their future : Proceedings of the seminar*. Yokohama, Japan.

Larocca, A. P. C., Schaal, R. E., Santos, M. C., & Langley, R. B. (2005). Monitoring the deflection of the pierre-laporte suspension bridge with the phase residual method. *Proceedings of the 18th International Technical Meeting of the Satellite Division of The Institute of Navigation, ION GNSS 2005*, *2005*(September), 2023–2028.

Mashaly, E. S., Ebrahim, T. M., Abou-Elfath, H., & Ebrahim, O. A. (2013). Evaluating the vertical vibration response of footbridges using a response spectrum approach. *Alexandria Engineering Journal*, *52*(3), 419–424. https://doi.org/10.1016/j.aej.2013.06.003

Psimoulis, P., Pytharouli, S., Karambalis, D., & Stiros, S. (2008). Potential of Global Positioning System (GPS) to measure frequencies of oscillations of engineering structures. *Journal of Sound and Vibration*. https://doi.org/10.1016/j.jsv.2008.04.036

Schaal, R. E., & Larocca, A. P. C. (2002). A Methodology for Monitoring Vertical Dynamic Sub-Centimeter Displacments with GPS. *GPS Solutions*. https://doi.org/10.1007/PL00012895

Strode, P. R. R., & Groves, P. D. (2016). GNSS multipath detection using three-frequency signal-to-noise measurements. *GPS Solutions*, *20*(3), 399–412. https://doi.org/10.1007/s10291-015-0449-1

Subirana, J. S., Zornoza, J. J., & Hernandez-Pajares, M. (2011). Fundamentals: GNSS Signal. Retrieved March 5, 2019, from https://gssc.esa.int/navipedia/

Teunissen, P. J. G., & Montenbruck, O. (2017). *Springer Handbook of Global Navigation Satellite Systems*. (P. J. G. Teunissen & O. Montenbruck, Eds.) (1st ed.). Berlin, Heidelberg: Springer International Publishing. https://doi.org/10.1007/978-3-319-42928-1

Vazquez B., G. E., Gaxiola-Camacho, J. R., Bennett, R., Guzman-Acevedo, G. M., & Gaxiola-Camacho, I. E. (2017). Structural evaluation of dynamic and semi-static displacements of the Juarez Bridge using GPS technology. *Measurement: Journal of the International Measurement Confederation*. https://doi.org/10.1016/j.measurement.2017.06.026

Xi, R., Jiang, W., Meng, X., Chen, H., & Chen, Q. (2018). Bridge monitoring using BDS-RTK and GPS-RTK techniques. *Measurement: Journal of the International Measurement Confederation*. https://doi.org/10.1016/j.measurement.2018.02.001

Yi, T. H., Li, H. N., & Gu, M. (2013). Experimental assessment of high-rate GPS receivers for deformation monitoring of bridge. *Measurement: Journal of the International Measurement Confederation*. https://doi.org/10.1016/j.measurement.2012.07.018

Yigit, C. O., Coskun, M. Z., Yavasoglu, H., Arslan, A., & Kalkan, Y. (2016). The potential of GPS Precise Point Positioning method for point displacement monitoring: A case study. *Measurement: Journal of the International Measurement Confederation*. https://doi.org/10.1016/j.measurement.2016.05.074